

Total ablation of the debris from the 1908 Tunguska explosion

V. V. Svetsov

Institute for Dynamics of Geospheres, Russian Academy of Sciences, 38 Leninskii Prospect, Moscow 117979, Russia

THE origin of the explosion over Tunguska, central Siberia, in 1908 has long been an enigma. Models^{1–3} of the disruption of solid objects entering the atmosphere indicate that the Tunguska explosion occurred at an altitude of 6–10 km, and that the source object was probably a stony asteroid⁴. But important questions concerning the nature of the object remain^{5,6}, particularly as no fragments have been identified in the area of the explosion. Unlike smaller objects (such as meteorites), which decelerate high in the atmosphere and can thus escape complete ablation and/or pulverization⁷, a Tunguska-sized object penetrates deeper into the atmosphere, where it will experience a greater aerodynamic load: the object should be disrupted into a vast number of fragments, each no larger than about 10 cm (ref. 2), which are then widely dispersed. Here I calculate the flux of radiation both inside and outside the fireball associated with the fragmenting object, and show that this is sufficient to totally ablate the dispersing fragments. The apparent absence of solid debris is therefore to be expected following the atmospheric fragmentation of a large stony asteroid.

On 30 June 1908, an unknown cosmic body came down to Earth in the basin of the Podkamennaja Tunguska, central Siberia. The main characteristics of the explosion—coordinates of epicentre, height, and energy yield (10–20 megatons)—have been deduced from seismic and atmospheric wave records and data on forest devastation. The absence of craters and meteorite fragments was easily explained by a cometary hypothesis, but theoretical investigations show that a representative comet of appropriate kinetic energy would explode too high in the atmosphere^{1,2}. Cometary origin, however, cannot be fully rejected because the trajectory inclination and entry velocity of the Tunguska object, as well as the density and composition of comets, are uncertain. Proponents of asteroidal origin of the Tunguska bolide inevitably imply that this impactor broke up and was pulverized in the atmosphere⁸. To investigate the problem quantitatively, it is necessary to estimate the sizes of the bolide fragments and radiation flux on them.

Korobeinikov *et al.*⁹ computed the radiation impulse on the ground on the assumption that the Tunguska event was a combination of spherical and cylindrical (with constant specific energy) explosions. The model of Chyba *et al.*⁴ gives energy release along the trajectory which can be treated as a line source of variable

specific energy $E(l)$, where l is the coordinate measured along the trajectory. The radiation flux at some point \mathbf{r} can be approximated as

$$q(\mathbf{r}, t) = \int_0^{L(t)} f(l, t) E(l) \frac{\cos \alpha}{4\pi D^2} e^{-k \int_0^D d ds} dl \quad (1)$$

where t is time, L the length of the trajectory, f the portion of energy radiated per unit time, D the distance from the trajectory point to \mathbf{r} , α the angle between the normal in relation to the illuminated surface and the ray directed to the trajectory point, k the averaged absorption coefficient of the undisturbed atmosphere¹⁰, d the ratio of atmospheric density to that at the sea level and s the coordinate along the ray. It was assumed that this function is identical to that of a cylinder-shaped explosion initiated by a cylinder enlarging its radius—the velocity and the maximum radius of the cylinder being equal to those of the meteoroid. Radiation transfer was computed with a multi-group approximation¹¹.

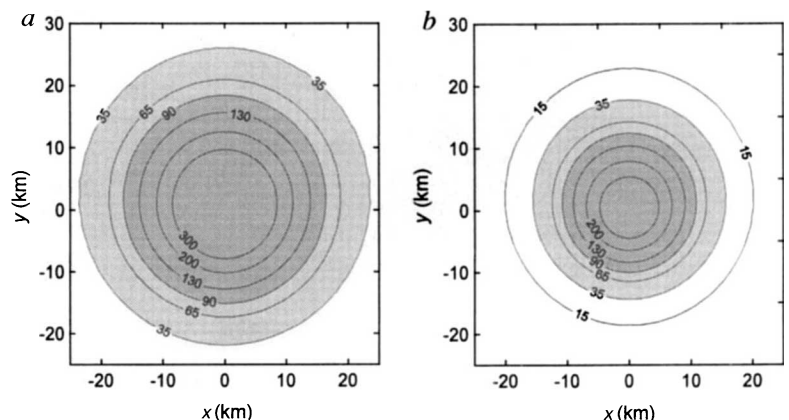
The calculations were made for 15-megaton asteroid-like object⁴ with an initial velocity of 15 km s^{-1} and an incidence angle of 45° . Maximum radiant exposure at the ground is shown in Fig. 1. The expeditions in the 1920s and 1930s reported that the average radius of the area of charred trees and soil was $\sim 15 \text{ km}$ with a scorch spread of up to $\sim 20 \text{ km}$, gradually decreasing at large distances^{12–14}. Computations for fine weather are consistent with these findings—about $40\text{--}60 \text{ J cm}^{-2}$ are required for visible charring of wood¹⁰.

Intense light flashes have been registered by satellite-based optical sensors^{15,16}. In this connection, a light curve of the Tunguska event seen from an infinite distance has been computed (Fig. 2). Growth rate of the main impulse is in line with the most powerful of the registered flashes, which additionally supports the idea of a pancake spreading impactor⁴.

Nevertheless, the behaviour of a heavily fragmented meteoroid is not so simple as the semi-analytic models^{1–4} predict. Rayleigh–Taylor instabilities (growing at the rate the idealised pancake impactor grows) lead to disintegration and spreading of the fluid impactor. Hydrocodes show that the meteoroid takes an irregular shape^{17,18} and fully pulverizes at some point in time¹⁸ and repulsive forces acting between the fragments^{19,20} produce a swarm of debris. Some results of hydrodynamic modelling¹⁸ for the late stage of disintegration are demonstrated in Fig. 3.

Fragmentation starts at a height of 25 km when the ram pressure exceeds the yield strength⁴. The pressure reaches its peak, $8 \times 10^8 \text{ dyn cm}^{-2}$, at about 10 km. Let us assume: (1) that the strength of the object diminishes with increasing size (scaling effect)^{21,22}; (2) the strength of centimetre stony samples is $1\text{--}6 \times 10^8 \text{ dyn cm}^{-2}$ (ref. 23); and (3) that smaller fragments lag behind²² while large ones take on the brunt of the aerodynamic load. Then, equating the fragment strength to the maximum

FIG. 1 Isolines of radiation energy absorbed by a unit area at the ground in J cm^{-2} . It is assumed that the irradiated surface is best orientated to accept the maximum radiation, that is, the isolines indicate a zone with the greatest possible heat damage. Results of computations are shown for atmospheric visibility up to a, 40 km (very clear, $k = 0.1 \text{ km}^{-1}$ (ref. 10)) and b, for the visibility of 20 km (clear, $k = 0.2 \text{ km}^{-1}$). The shaded area lies within the threshold for setting fires. The y-axis is a projection of the bolide trajectory to the Earth's surface. The coordinates start at the epicentre—the z-axis meets the trajectory at an altitude of 7 km. The computational results give the best fit to the evidence^{12–14} at weather conditions between very clear and clear. The maximum radiant exposure at 70 km to the south-east is 0.55 J cm^{-2} for 40 km visibility and 0.033 J cm^{-2} for 20 km visibility. That is also in reasonable agreement with eyewitness reports from Vanovara²⁹.



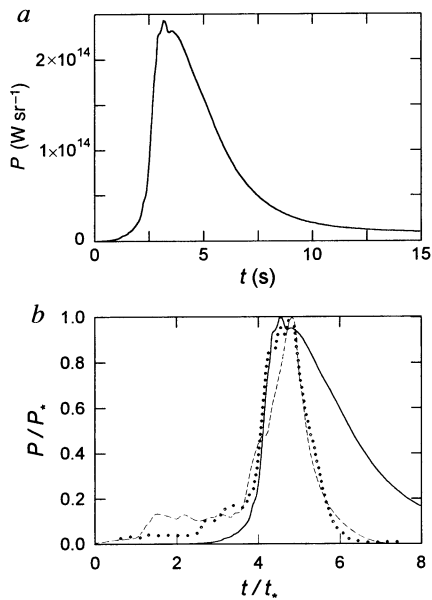


FIG. 2 a, Radiation power per unit solid angle versus time as it would be seen from a satellite viewing the Tunguska explosion. b, The Tunguska radiation impulse is compared with events registered by satellite based sensors on 1 October 1990 (dotted line) and 1 February 1994 (dashed line). The following nondimensional units are used in the latter case: P is the maximum of radiation power, t is the scale time equal to E/P , where E is the energy radiated from the beginning of the impulse till its peak. Growth rates of the main flashes differ insignificantly. A rise in light power before the main flash in the registered light curves shows that the breakup can go through several stages. The Tunguska light curve decline rate is lower because of the much higher energy and a lesser altitude of the Tunguska explosion. Initial kinetic energies of the impactors were about 6 kilotons and 40 kilotons in the 1 October 1990 and the 1 February 1994 events respectively, assuming a 10% conversion of kinetic energy to radiation energy¹⁶. The source height at peak power is about 30 km for the 1 October 1990 and about 21 km for the 1 February 1994 events. A calculated coefficient of conversion for kinetic energy to radiation for the hypothetical Tunguska event is 20%, twice that for the events with smaller energy due to much longer decline part of the light curve. The whole impulse lasts for about 20 s in agreement with observational data for powerful nuclear explosions in the atmosphere¹⁰. The radiation efficiency of the Tunguska bolide is much higher than empirical radiation efficiencies for small meteors³⁰ (~1%) due to greater optical thickness of the Tunguska fireball, but it is lower than thermal partition of a nuclear explosion^{10,31} (35–43%) owing to lower temperatures. Dust and vapour, especially metallic components, may change the opacities and radiation efficiencies obtained here.

FIG. 3 A swarm of debris at full disintegration stage of the Tunguska meteoroid. Numerical results were initially obtained for a 2-km fragment of the comet Shoemaker–Levy 9 (ref. 18) and then converted to the 58-m Tunguska object on the assumption of hydrodynamic similarity and the pancake model applicability. Dramatic deceleration occurs within a much shorter distance than the scale height of the atmosphere for both of the events. Solid circles are particles of the meteoroid, points are particles of the atmosphere. The regular pattern of points corresponds to the undisturbed atmosphere. The hypothetical meteoroid initially consisted of 650 particles, but only 340 particles are confined to computational region shown in the figure. The rest are decelerated in the far wake. Particles located between leading fragments and the cross-section at a 300 m distance from it have, in average, 65% of the initial velocity, that is $\sim 10 \text{ km s}^{-1}$. More massive fragments hold a leading position. The meteoroid breakdown into small segregated debris suggests a large increase in the total surface. Ablation rate at the disintegration stage becomes much greater than the single-body models^{2,4,5} predict.

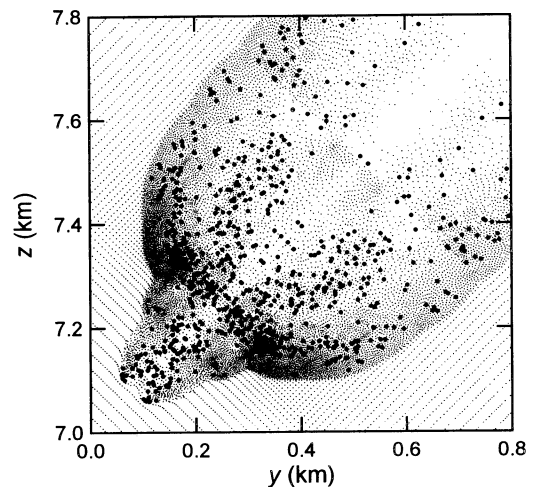
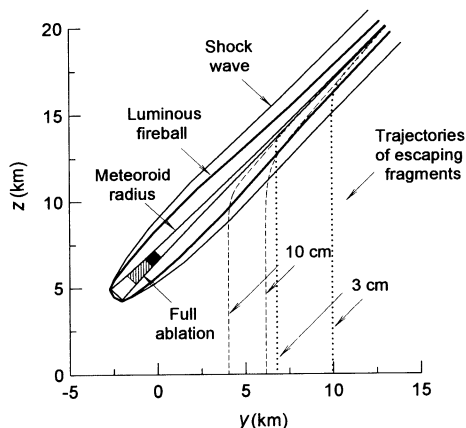


FIG. 4 The shape of the shock wave and the fireball; the bolide's head velocity is down to 3 km s^{-1} . The computational results are obtained using the spreading impactor model⁴ and treating the energy release as a linear source. The increasing radius of meteoroid is plotted inside the fireball. The luminous region boundary is defined as an isotherm of 2,500 K temperature. Computations of fragment motion and ablation show that 3-cm fragments fully ablate as they begin to move separately inside the area shown by hatching. Fragments 10 cm in size ablate if they are segregated inside or above the shaded area. Above the shaded zone, the bolide is heavily fragmented but the fragments are not completely dispersed. It is highly probable that the dispersion occurs at the upper boundary of the shaded region. Trajectories of fragments that escape the fireball at altitudes of 15 to 20 km at a lateral velocity of 1 km s^{-1} are shown by dashed lines for 10-cm fragments and by dotted lines for 3-cm fragments. It is possible that remnants of such fragments could reach the ground at a distance of 5 to 10 km from the epicentre. Fragments 3 cm in size escaping the fireball at altitudes below 14 km do not survive the fall because of the sufficiently high radiation flux (about 10^5 W cm^{-2}) on their surface. Larger (10 cm) fragments escaping from the fireball at altitudes below 15 km could withstand radiation from the fireball. It is unlikely, however, that they survive because they are weaker (because of the scaling effect) and would be broken up at aerodynamic loads greater than $4 \times 10^8 \text{ dyn cm}^{-2}$.



pressure, we find that sizes of surviving fragments are less than 1–3 cm. A fragmentation model of Hills and Goda² at constant strength predicts the largest fragment mass to be ~ 1 kg, which implies that the fragment size is under 10 cm for the stony impactor considered here.

Change in mass, m , of a single fragment is given by

$$Q \frac{dm}{dt} = -qA \quad (2)$$

where Q is the heat of ablation, q the radiation flux density on the surface, and A the surface area—full surface if the fragment is entirely immersed in the fireball, or cross-section if it is irradiated from one side. Despite the fact that $Q = 8 \text{ kJ g}^{-1}$ on vaporization, a value of $Q = 2 \text{ kJ g}^{-1}$ is more suitable for meteoroids owing to instabilities in melted layers, inhomogeneities, and existence of volatiles in stony meteoroids²⁴ (the heat transfer coefficient, commonly involved in equation (2), is not used here because q is evaluated directly.) For a fragment inside the swarm, q is about the radiation flux of black-body with a temperature equal to that behind the shock wave of the swarm if the velocity is from 10 km s^{-1} to 4 km s^{-1} . Free paths of photons are from 0.1 cm to 100 m in this case²⁵, less than the fireball size but greater than the screening layer around the fragment. Free paths of photons depend on the temperature and density of the air. For velocities below 10 km s^{-1} , the temperatures are less than 15,000 K, the air is partially ionized and the opacities are determined mainly by bound-free and free-free electron transitions. Screening by vapour is negligible because the vapour mainly absorbs hard photons, with energies above 7.5 eV (ref. 26).

Some fragments can escape the fireball as a result of accidental collisions. The radiation flux q is then determined by equation (1) if the fragment velocity falls below 7 km s^{-1} —the effect of screening of soft fireball radiation by the shock-heated cap around the fragment disappears. If we take up these assumptions, the computations show that 3–10 cm fragments fully ablate inside or outside the fireball unless the altitude at which they gain significant lateral velocity is high enough (Fig. 4). Conceivably, micro-sized particles trapped by resin of trees^{27,28} might be recondensed material precipitated in the general vicinity of the impact site. Similar to the impact of the comet Shoemaker–Levy 9, Tunguska debris was probably also widely scattered because of the wake, a rarefied channel made by the bolide in the atmosphere. Two essential properties of a large bolide lead to the result reported here: fragment sizes are much less than they are for small impactors and, second, radiation energy is decidedly large—quite comparable with that of a nuclear explosion. \square

Received 17 May; accepted 3 September 1996.

- Zahnle, K. J. *J. Geophys. Res.* **97**, 10243–10255 (1992).
- Hills, J. G. & Goda, M. P. *Astron. J.* **105**, 1114–1144 (1993).
- Grigoryan, S. S. *Cosmic. Res.* **17**, 724–740 (1979).
- Chyba, C. F., Thomas, P. J. & Zahnle, K. J. *Nature* **361**, 40–44 (1993).
- Lyne, J. E. & Tauber, M. *Nature* **375**, 638–639 (1995).
- Bronshten, V. A. & Zotkin, I. T. *Sol. Syst. Res.* **29**, 241–245 (1995).
- Wetherill, G. W. & ReVelle, D. O. *Icarus* **48**, 308–329 (1981).
- Secanina, Z. *Astron. J.* **88**, 1382–1414 (1983).
- Korobeinikov, V. P., Chushkin, P. I. & Shurshalov, L. V. *Acta Astron.* **9**, 641–643 (1982).
- Glasston, S. & Dolan, P. J. *The Effects of Nuclear Weapons* (Govt Printing Office, Washington DC, 1977).
- Svetsov, V. V. *Comp. Maths Math. Phys.* **34**, 365–376 (1994).
- Kulik, L. A. *Dokl. Akad. Nauk* **22**, 520–524 (1939).
- Kulik, L. A. in *Voprosi Meteoritiki* 15–19 (Tomsk University, Tomsk, 1976).
- Krinov, E. L. *Giant Meteorites* (Pergamon, Oxford, 1966).
- Tagliaferrri, E., Spalding, R., Jacobs, C., Worden, S. P. & Erlich, A. in *Hazards due to Comets and Asteroids* (ed. Gehrels, T.) 199–220 (Univ. Arizona Press, Tucson, 1994).
- McCord, Jh. B. et al. *J. Geophys. Res.* **100**, 3245–3249 (1995).
- MacLow, M.-M. & Zahnle, K. J. *Astrophys. J.* **434**, L33–L36 (1994).
- Svetsov, V. V. *Sol. Syst. Res.* **29**, 331–340 (1995).
- Passey, Q. R. & Melosh, H. J. *Icarus* **42**, 211–233 (1980).
- Melosh, H. J. *Impact Cratering: A Geologic Process* (Oxford Univ. Press, New York, 1989).
- Tsvetkov, V. I. & Skripnik, A. Ya. *Sol. Syst. Res.* **25**, 273–279 (1991).
- Svetsov, V. V., Nemtchinov, I. V. & Teterov, A. V. *Icarus* **116**, 131–153 (1995).
- Medvedev, R. V., Gorbatshevich, F. F. & Zotkin, I. T. *Meteoritika* **44**, 105–110 (1985).
- Bronshten, V. A. *Sol. Syst. Res.* **29**, 392–399 (1995).
- Avilova, I. V., Biberman, L. M. et al. *Optical Properties of Hot Air* (Nauka, Moscow, 1970).
- Biberman, L. M., Bronin, S. Ya. & Brykin, M. V. *Acta Astron.* **7**, 53–65 (1980).
- Longo, G., Serra, R., Cecchini, S. & Galli, M. *Planet. Space Sci.* **42**, 163–177 (1994).
- Korlevic, K. & Valdré, G. *Planet. Space Sci.* **42**, 791–792 (1994).
- Kulik, L. A. *Dokl. Akad. Nauk, Ser. A* **23**, 399–402 (1927).

- Bronshten, V. A. *Physics of Meteoric Phenomena* (Reidel, Dordrecht, 1983).
- Svetsov, V. V. *Combustion Explosion and Shock Waves* **30**, 696–707 (1994).

ACKNOWLEDGEMENTS. I thank V. Shuvalov and V. Fartushny for useful discussions, and L. Beletskaya for technical assistance. This work was supported by Sandia National Laboratories.

CORRESPONDENCE should be addressed to V.V.S. (e-mail: idg@glas.apc.org).

Two-dimensional photonic-bandgap structures operating at near-infrared wavelengths

Thomas F. Krauss*, Richard M. De La Rue* & Stuart Brand†

* Optoelectronics Research Group, Department of Electronics and Electrical Engineering, University of Glasgow, Glasgow G12 8LT, UK

† Department of Physics, University of Durham, Durham DH1 3LE, UK

PHOTONIC crystals are artificial structures having a periodic dielectric structure designed to influence the behaviour of photons in much the same way that the crystal structure of a semiconductor affects the properties of electrons¹. In particular, photonic crystals forbid propagation of photons having a certain range of energies (known as a photonic bandgap), a property that could be incorporated in the design of novel optoelectronic devices². Following the demonstration of a material with a full photonic bandgap at microwave frequencies³, there has been considerable progress in the fabrication of three-dimensional photonic crystals with operational wavelengths as short as 1.5 μm (ref. 4), although the optical properties of such structures are still far from ideal⁵. Here we show that, by restricting the geometry of the photonic crystal to two dimensions (in a waveguide configuration), structures with polarization-sensitive photonic bandgaps at still lower wavelengths (in the range 800–900 nm) can be readily fabricated. Our approach should permit the straightforward integration of photonic-bandgap structures with other optical and optoelectronic devices.

The main factors that determine the properties of photonic-bandgap (PBG) structures are the refractive-index contrast, the fraction of high- and low-index materials in the lattice and the arrangement of the lattice elements. Band-structure calculations show that lattices arranged like a ‘honeycomb’^{6,7} or like the atoms in a ‘graphite’^{7,8} structure are the most favoured arrangements and predict that the widest bandgap occurs when small regions of high-index semiconductor are surrounded by large regions of air, that is, when the semiconductor ‘area fill-factor’ is low.

In two-dimensional structures, an additional factor is light confinement; either (1) the structure must be big compared to the beam size or (2) the beam must be sufficiently confined within a waveguide to allow the multiple coherent back-reflections that are required for a PBG. Considering the difficulty of defining periodic structures with sub-100-nm feature sizes, it is beyond current technological capabilities to translate such a pattern into a dielectric matrix many wavelengths deep, so solution (1) is currently not possible at optical wavelengths. Solution (2) has already been realized with semiconductor waveguides^{9–11} and was adopted here.

The waveguide configuration used is comparable to that of a semiconductor laser⁹. A matrix of very small (~ 100 nm diameter) holes was etched into the waveguide, through the guiding core, to form a honeycomb lattice (Fig. 1). The main difference between our approach and that of others is that the semiconductor area fill-factor is high, so light is confined by a waveguide over most of the propagation path and the strong PBG effects can take place although the depth of the structure is less than the free-space wavelength. If, instead, we adopted the large air-fill factor lattices suggested by theory, the light would only be guided in a small part